HSLA Steels 2015, Microalloying 2015 & Offshore Engineering Steels 2015
The Chinese Society for Metals (CSM) and Chinese Academy of Engineering (CAE)
TMS, 2016

MICROALLOYED STEELS: PAST, PRESENT AND FUTURE

Anthony J. DeArdo

Director of Basic Metals Processing Research Institute
Department of Mechanical Engineering and Materials Science
Swanson School of Engineering, University of Pittsburgh, Pittsburgh, PA 15261, USA
And also
Finland Distinguish Professor
Department of Mechanical Engineering
University of Oulu

Keywords: HSLA Steels, Microstructure, Recrystallization, Thermomechanical Processing

Abstract

The role of microalloying has changed over the years as the range of products where used has expanded and the production processes have improved. When used in the early ferrite-pearlite steels, its chief function was grain refinement and precipitation hardening. Later, as the quest for higher strength led to bainitic and martensitic microstructures, the role of microalloying changed to grain refinement and transformation control. Later still microalloying has been successfully applied in martensitic and the advanced high strength steels grades for automobiles. The goal of this paper is to follow this changing role of microalloying in both conventional and advanced steels from the 1960s until today.

Introduction

Although there has always been a demand for high strength flat rolled steel, the interest in higher strength steels increased in the 1970s as a result of the global economic dislocation caused by the Oil Embargos in the Middle East. The development of modern microalloyed HSLA steels began in the early 1970s when the world suffered the first of two crises in its oil supply from the Middle-East. These events led to a quadrupling of the crude oil prices on oil imported from that area, and resulted in a decade-long abnormal increase in oil prices. This disruption had a large impact on the global economy and the steel industry, in particular. Whereas the concepts of downsizing or light weighting were an afterthought in steel usage in the 1960s, they became the mantra of the steel industry after the Oil Embargo of 1973.

Prior to 1973, the global steel industry produced mainly lower strength ferrite-pearlite steels for general use and small amounts of martensitic heat treated steels when higher strengths and hardness were required. However, after the price of oil skyrocketed, much attention was focused on downsizing and light weighting by practically every industry, but most particularly in the transportation industries, construction and of course in the oil industry. However, downsizing and light weighting can only occur by the use of higher strength steels, where thinner gages can be used. Heat treated steels were not the answer as the heat treating facilities were rather limited, and being a batch process, further limited productivity. The answer was high strength hot rolled steel, where the steel had the required properties after being cooled or coiled to room temperature, e.g., with YS > 420MPa. These hot rolled steels could be produced efficiently in large tonnages. The central question at that time was how to produce high strength hot rolled steels without heat treatment. As is now well-known, these steels also had to be strong, tough and weldable.

Since the early plate mills had mainly only air cooling after rolling, the early steels had ferrite-pearlite microstructures with modest strengths at 12-20mm gauge as discussed above. As the operating pressures and pipe diameters continued to increase, and the wall thickness decrease, the stresses in the pipe wall also increased. This required the use of even higher strength steels.

Research over the past half-century has led to the availability of steels with YS ranging from 350 to 1000 MPa for use in the transportation, construction and energy industries. This paper attempts to document some of the milestones on the road from simple C-Mn-Si hot rolled steels of the 1960s with ferrite-pearlite (F-P) microstructures to the modern bainitic, martensitic and multi-phase steels of today and tomorrow. Much of this improvement has been enabled by improvements in steelmaking, hot rolling and cooling technologies, but equally important has been the critical role of microalloying in this evolutionary development.

Microalloying and Ferrite-Pearlite Steels in the Strength Range of YS 350-500 MPa

After nearly a half-century of research, it is now clear that microalloying additions play several roles in all HSLA, but in particular in those steels with ferrite-pearlite microstructures. Their chief function is to control: (a) austenite conditioning for grain refinement, (b) lower the transformation temperature, and (c) possibly cause precipitation hardening. They do so by controlling the critical temperatures of the austenite such that they can be adjusted to meet the characteristics of the processing equipment and also the properties of the final product. These critical temperatures are: (i) the grain coarsening temperature during reheating, (ii) the recrystallization stop temperature during hot rolling and (iii) the transformation temperature during cooling [1-3]. These effects are shown schematically in Figure 1 superimposed on the Fe-Fe_3C phase diagram.

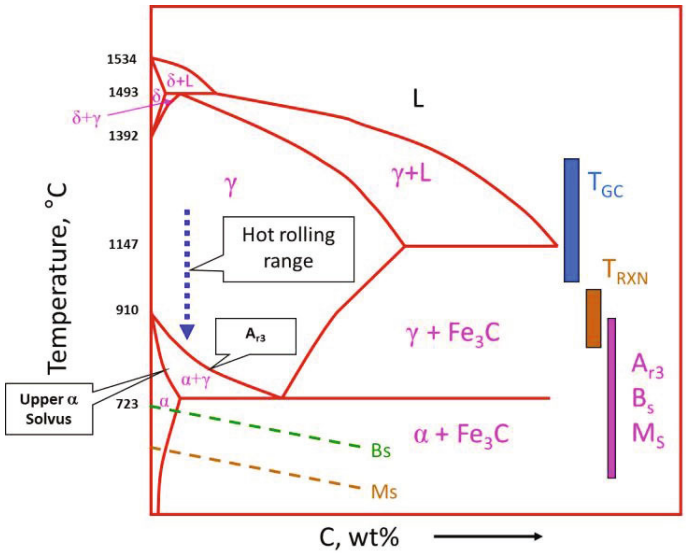

Figure 1. Fe-C phase diagram, with critical temperatures indicated

The transformation temperature of a steel is governed by its hardenability or CCT diagram and the operative cooling rate. When this temperature is above 650C with steels of moderate Mn content, the resulting microstructure is ferrite-pearlite. It is well-known that the strength of F-P steels can be expressed by the expanded Hall-Petch equation [4], where the grain size effect and the precipitation hardening increment are dominant. An example is shown in Figure 2. Plain

carbon steels with polygonal ferrite-pearlite microstructures and with a ferrite grain size of approximately 6 microns, should have a YS of about 400 MPa and a UTS of approximately 500 MPa, while a microalloyed steel of similar grain size might have a YS higher by 100MPa. Even higher strengths are achievable if the ferrite is quasi-polygonal or slightly acicular in nature, or if there is a significant contribution from precipitation hardening.

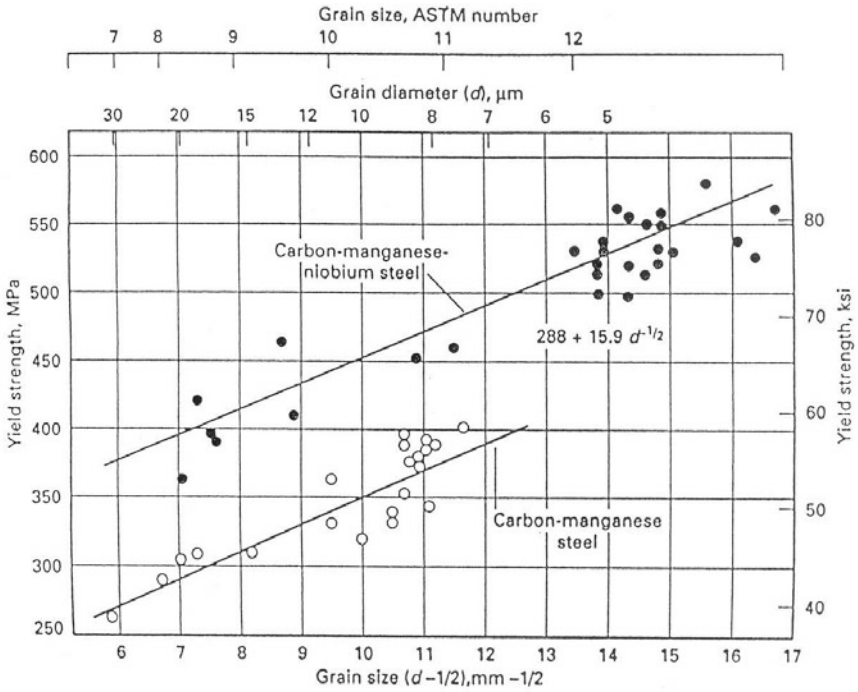

Figure 2. Experimental Hall-Petch relationships as determind by quantitative metallograph for carbon-manganese and carbon-manganese-nioblum steels.

Microalloying and Austenite Conditioning

Since the as hot rolled austenite grain size is so critical to the final microstructure, strength and toughness of MA HSLA steels after cooling, a good portion of the early research was focused on this aspect. A critical contribution to this area came from Kozasu who showed in 1975 that the effectiveness of the austenite grain structure can be indexed by the grain stereological parameter Sv [5]. The higher the Sv, the more grain boundaries and deformation bands per unit volume, and the more effective the austenite would be in nucleating ferrite and also in stopping the growth of cleavage cracks. The crystalline defects that comprise the Sv are shown in Figure 3 and the effect of Sv on FGS is shown in Figure 4 [6].

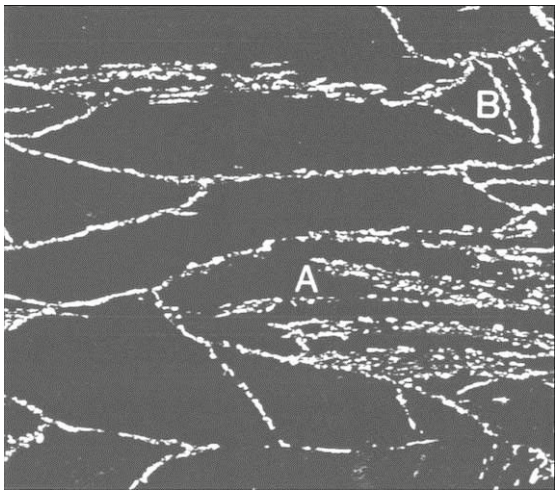

Figure 3. Dark field optical micrograph of nucleation of ferrite at deformed austenite grain boundaries, deformation bands (A), and annealing twins (B).

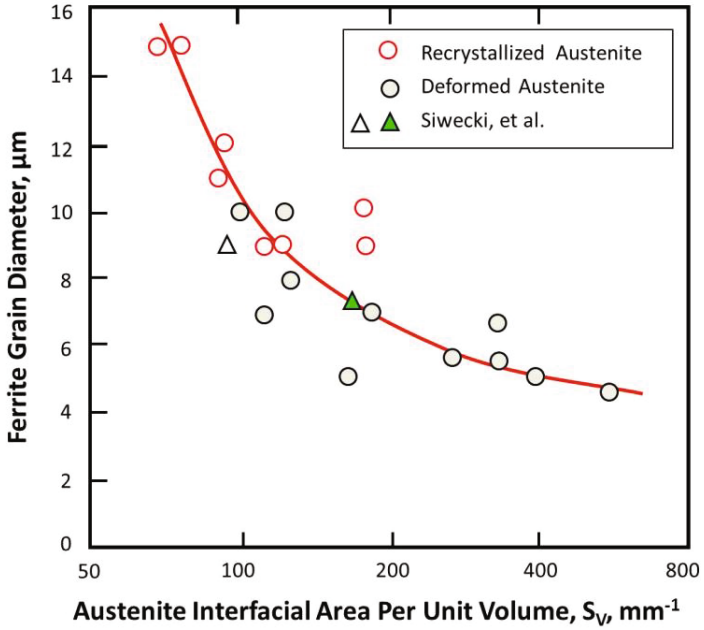

Figure 4. Ferrite grain sizes produced from recrystallized and recrystallized austenite at various S_v values.

It was shown that the role of microalloying in increasing Sv was to generate retarding forces that would slow or stop the static recovery or recrystallization that would otherwise occur between passes in the rolling mill. For plate mills with many light passes and long interpass times, the MA acted to suppress recrystallization by forming strain-induced precipitates that could pin the grain and subgrain boundaries. However, for strip mills with fewer, heavier passes and short interpass times, the MA would act to suppress recrystallization by exerting solute drag on the dislocations and sub-grain boundaries. Both Nb and V can be useful in this regards, although they do so over different temperature ranges, due to their different solubility products. The guiding principle learned from this early work is that the recrystallization stop temperature T5, as defined in Figure 5, can be controlled through microalloying and the MA addition should be selected to match the rolling practice of interest for the case of plate rolling[7]. The pancaked

grains that result from deforming below T5 are shown in Figure 6 for VAN steel [8]. The strain-induced precipitate responsible for the pinning force that had suppressed static recrystallization is shown in Figures 7 and 8, for V steel [8] and Nb steel [1], respectively.

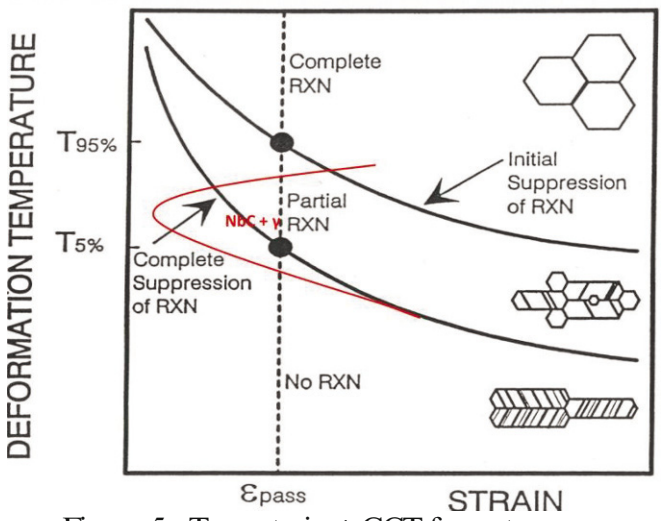

Figure 5. T vs strain + CCT for pptn curve

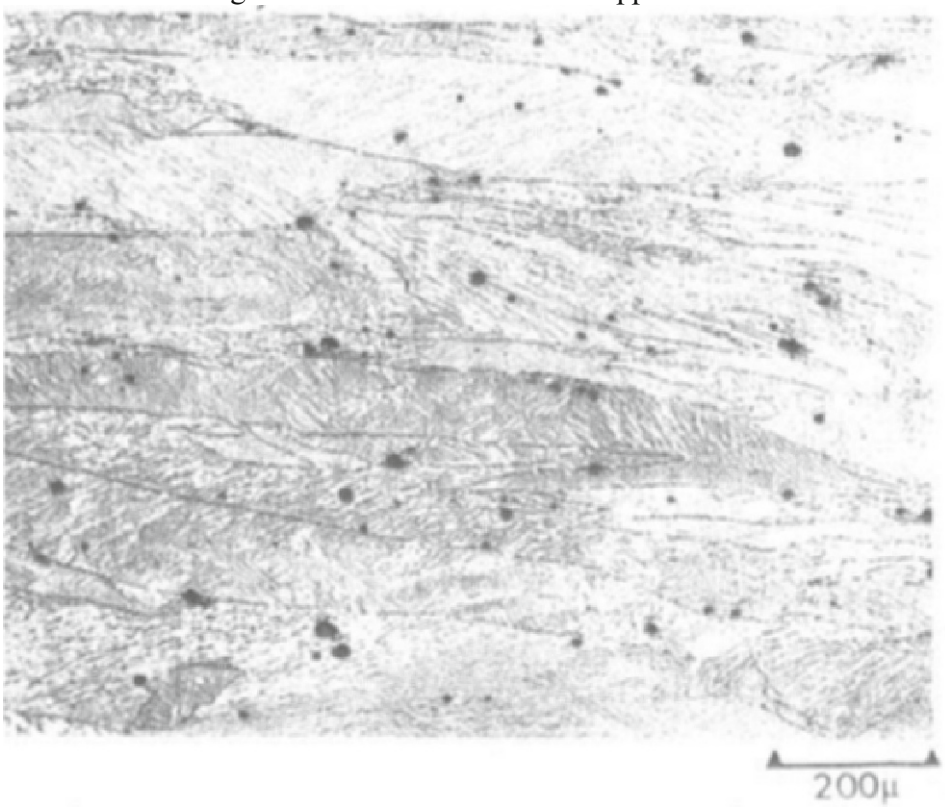

Figure 6. Optical micrograph of V steel hot rolled 50%, held 3 minutes at 1600°F, WQRT [5]

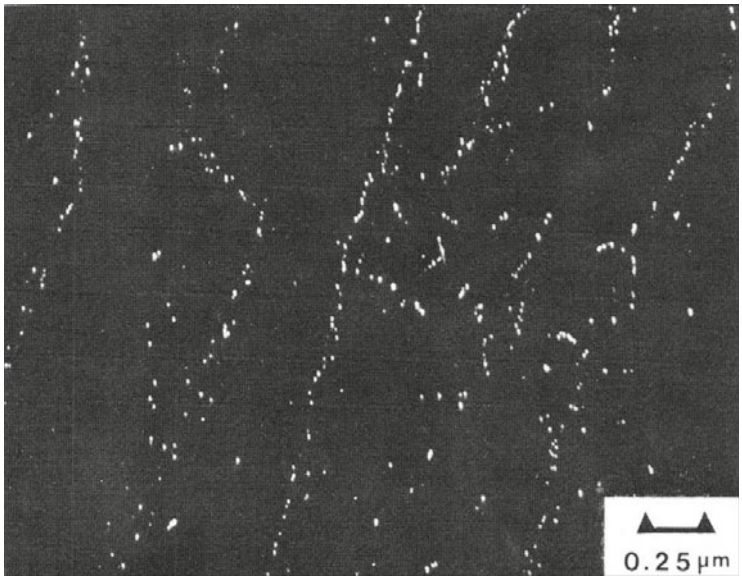

Figure 7. Dark field TEM micrograph taken with $110_{V(CN)}$ spot showing V(CN) precipitates on the subgrain boundaries of the prior austenite. Sample hot rolled 50% at 1600°F (871°C) and held 12 minutes, then air cooled to room temperature.[5]

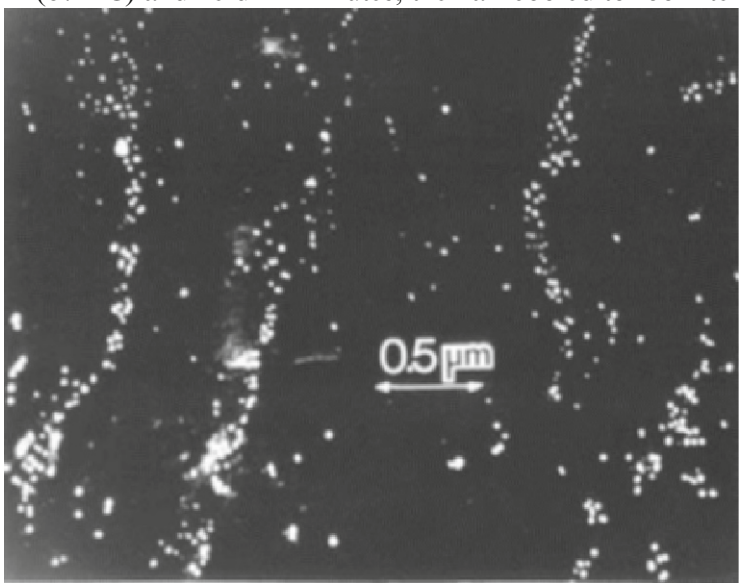

Figure 8. Strain induced precipitation of NbCN in austenite in a steel containing 0.09%C - 0.07%Nb. Specimen reheated at 1250°C, rolled 25% and held at 950°C, and air cooled to RT. Centered dark field electron micrograph using a (111) NbC reflection. After Santella, 1981.

However, knowing the tenants of the basic physical metallurgy is not the same as understanding how to use the knowledge in a steel plant. Fortunately, this era also produced some important diagrams that could be used in a practical sense to improve the MA HSLA steels, both in their compositions and their processing. The first of these is how the recrystallization stop temperature T5 can be controlled or pre-selected for a given steel or rolling mill. It was shown that the T5 temperature can vary with different MA precipitation systems in plate rolling experiments, Figure 9 [9]. This diagram illustrates how the T5 temperature can be pre-selected based on the steel, rolling process and the level of microalloying needed.

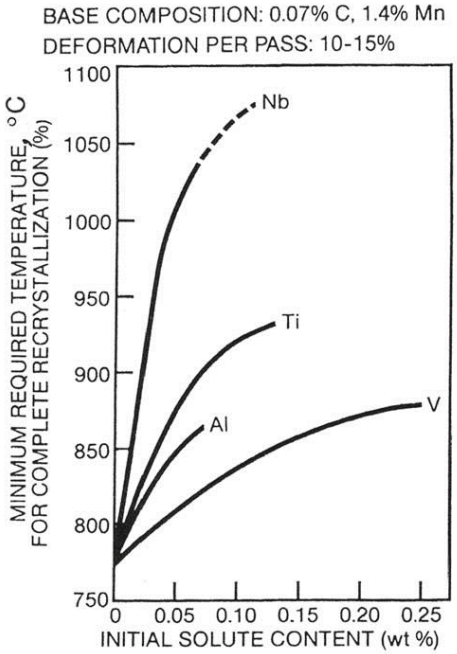

Figure 9. Retardation of austenite recrystallization by different alloying elements.[21]

Strength of Ferrite– Pearlite Microalloyed HSLA Steels

It is obvious from Figure 2 that the ferrite grain size makes a significant contribution to the strength of ferrite-pearlite steels. Although other strengthening mechanisms have been identified, e.g., solute hardening, texture hardening and dislocation hardening, only precipitation hardening was shown to be important in ferrite-pearlite microstructures. Research over thirty years from that era to the present showed repeatedly that there can be two forms of precipitates formed in ferrite leading to precipitation hardening, interphase precipitation at higher temperatures and slower cooling rates (10RWKH, 11Kirst, 12Todd, 13 Gao, 14Sweden, 15Spain), Figure 10 for a V steel (16Batte) and Figure 11 for a Nb steel (17Santella). However, general precipitation occurred in ferrite formed and held at lower temperatures, e.g., slow cooling from the water end temperature for rapidly cooled plates or lower coiling temperatures for strip. (11Sakuma, 12Kirsti, 18Cryderman, 14Sweden, 15Spain).

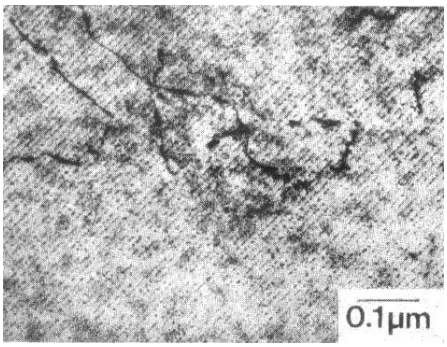

Figure 10. Bright field TEM of Interphase VCN in ferrite at 725C, Fe-0.75V-0.15C

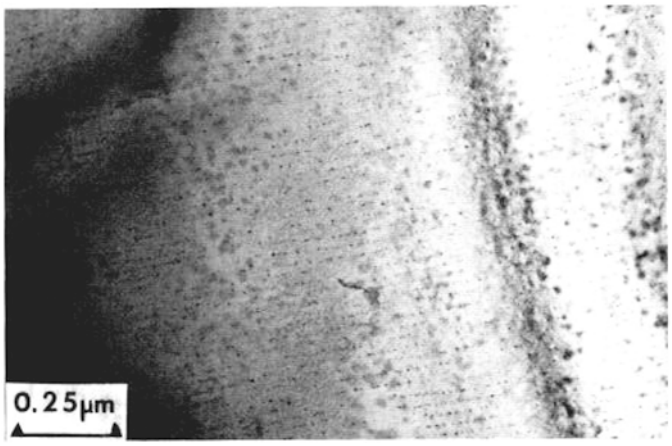

Figure 11. Interphase precipitation of NBCN in ferrite in steel containing 0.09%C - 0.07%Nb. Specimen was reheated to 1250°C, hot rolled to 1000°C and air cooled to RT. Bright field electron micrograph. After Santella, 1981.

Guidelines for selecting the overall composition of a steel for a given application including strength, toughness and weldability were also published at this time, and have been reviewed [1-3].

In summary, ferrite pearlite microstructures of microalloyed HSLA steels can achieve yield and strengths from 280 to about 500 MPa. in reasonable gages with good toughness and weldability.

Pathway to high strength steels

The route to higher strengths beyond those available with ferrite-pearlite microstructures was presented by Irvine and Pickering in the late 1950s, when they showed how the strength of bainitic steel was related to the transformation temperature, Figure 12[19].

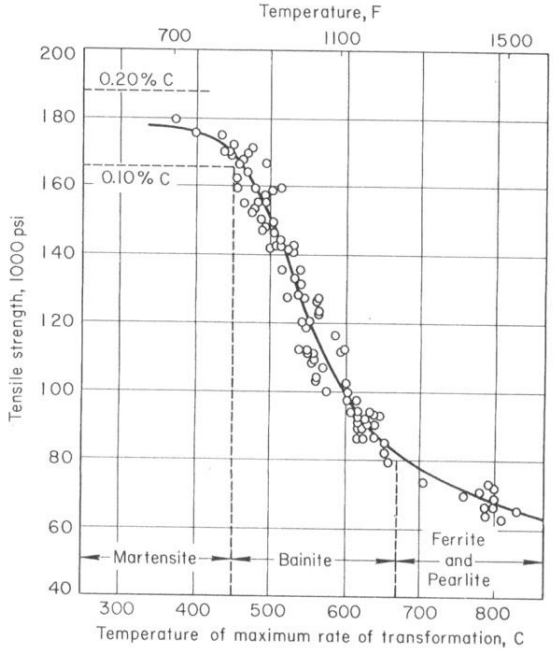

Figure 12. Effect of temperature of maximum transformation rate on tensile strength in a series of alloys with a base composition containing 0.5%Mo and 0.002%B. Cooling rate was typical of those obtained during air cooling of a 19 mm-diam bar. (irvine and Pickering)

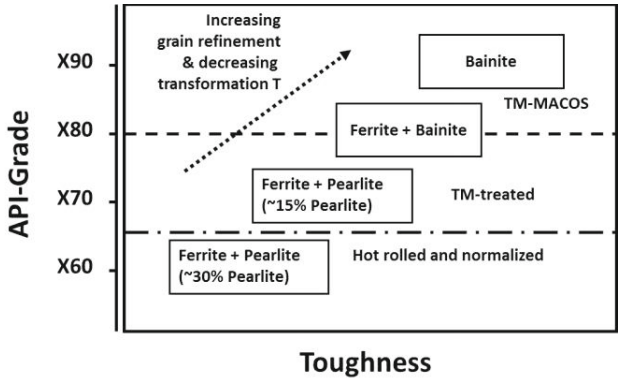

Figure 13. Evolution of plate steel for large diam. linepipe: microstructure and properties.

A similar concept was later presented in the context of plate rolling, Figure 13[20]

To reach higher strengths, the transformation temperature must be lowered by alloying and water cooling in the case of plate as shown in Figures 12 and 13, or by lowering the coiling temperature in the case of strip. For strip mill simulations, the influence of Mn-Cr-Mo-V were studied on the Bs and Bf temperatures during continuous cooling at 30°C/s, Figure 14 [21]. It is clear that the addition of V had a small effect on these temperatures and a larger effect in the presence of higher N.

Although the effect of the V or V-N on the Bs was not large, the resulting effect of coiling temperature on strength was quite impressive, Figure 15 [21].

The influence of alloying on the Bs and Bf temperatures in bainitic strip steels containing V or V-N is shown in Figure 14 [21].

There is more of a slope to the B_S and B_f lines in the Cr-Mo-V steel CCT diagrams, Fig.8. It is interesting to note that the addition of V or V-N to a 0.04C-1.3Mn-Cr-Mo steel had little apparent effect on the transformation temperatures, B_S and B_f, Fig.9, but did have a significant effect on mechanical properties when viewed from the coiling temperature in a ROT simulation, Fig.10 [21].

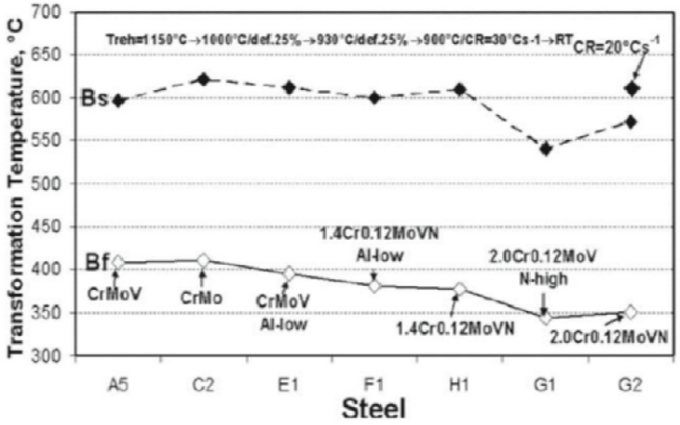

Figure 14. Effect of Cr, Mn, Mo, V, Al and N on transformation characteristics of deformed specimens during cooling at 30°C/s from 900°C to RT. The upper curve is the start temperature and the lower the finish temperature [21].

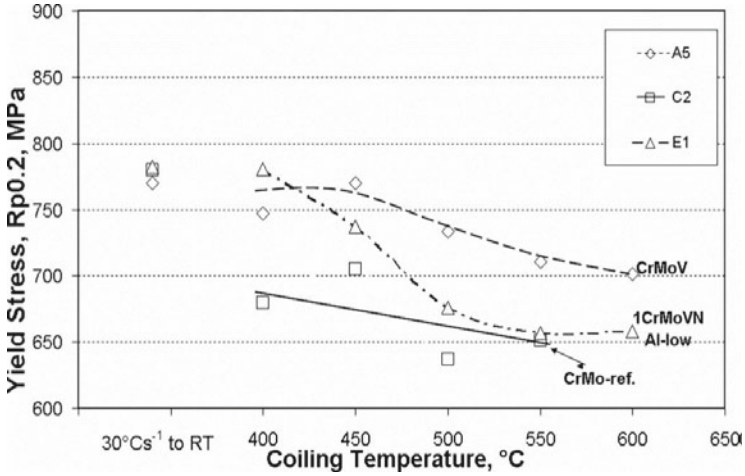

Figure 15. Yield stress versus coiling temperature for the steels with standard contents of 1% Cr and 0.25% Mo. Results for continuous cooling at 30°C/s to RT are also shown [21].

High Strength Bainite

In an attempt to reach yield strengths over 690 MPa in heavier plates, a steel of high C.E.(~0.5) and Pcm(~0.21) was investigated [22 – 24]. The composition is shown in Table 1.

Table 1. Steel Composition, wt%

C	Mn	P	S	Si	Cu +Ni +Cr+Mo	Ti	Al	N	Nb	B
0.06	1.89	0.009	0.0016	0.29	1.25	0.01	0.023	0.0046	0.039	0.0005

This steel was controlled rolled and then water spray cooled at 10C/s to either 400C (Steel B1) or 500C(Steel B2), then ACRT. The two specimens had similar tensile properties, but steel B1 had a DBTT of -60C while steel B2 showed -20C. The metallography conducted to help explain the difference in low temperature toughness revealed several important differences. First, the crystallographic packet size was smaller in B1 than in B2, Figure 16. Second, the amount and

size of the MA microconstituent were larger in B1 than in B2, Figure 17. And third, it should also be mentioned that given sufficient time, the repartitioning of carbon can occur leading to the reformation of austenite during the bainite reaction, resulting in higher carbon fresh martensite to form during the final cool. This untampered martensite is thought to contribute to lower toughness resulting from slower rates of cooling or extended isothermal holding times below the Bs temperature(Oulu, MST14, Met Trans)

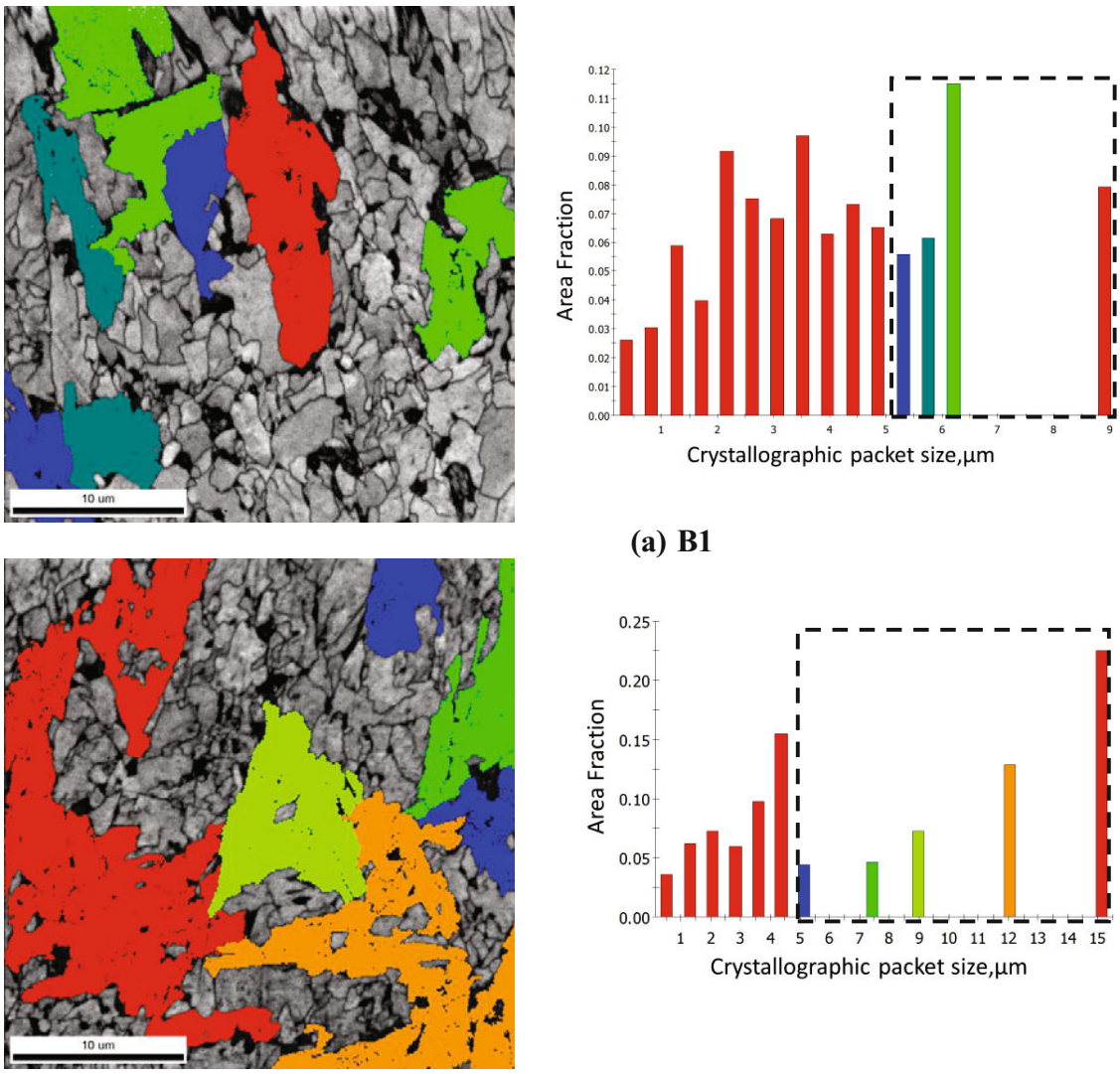

Figure 16. The highlighted crystallographic packets (left) and sizes (right) in a) sample B1; and b) sample B2.

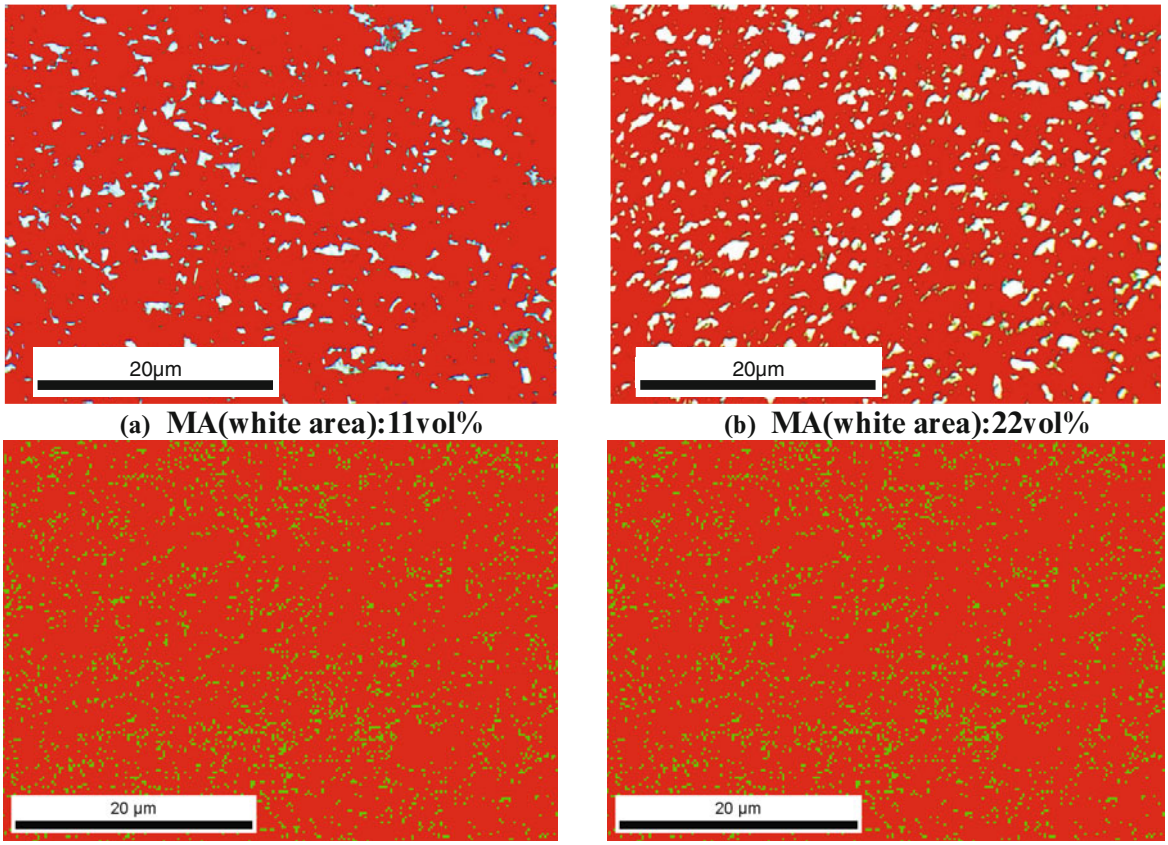

(a) MA(white area):11vol% **(b) MA(white area):22vol%**

(c) Retained austenite(green area):10vol% **(d) Retained austenite(green area): 8vol%**

Figure 17. The distribution of MA in samples B1: (left) (a) Image based on LePera etched microstructures, (c) EBSD analyzed retained austenite; and B2: (right) (b) Image based on LePera etched microstructures, (d) EBSD analyzed retained austenite.

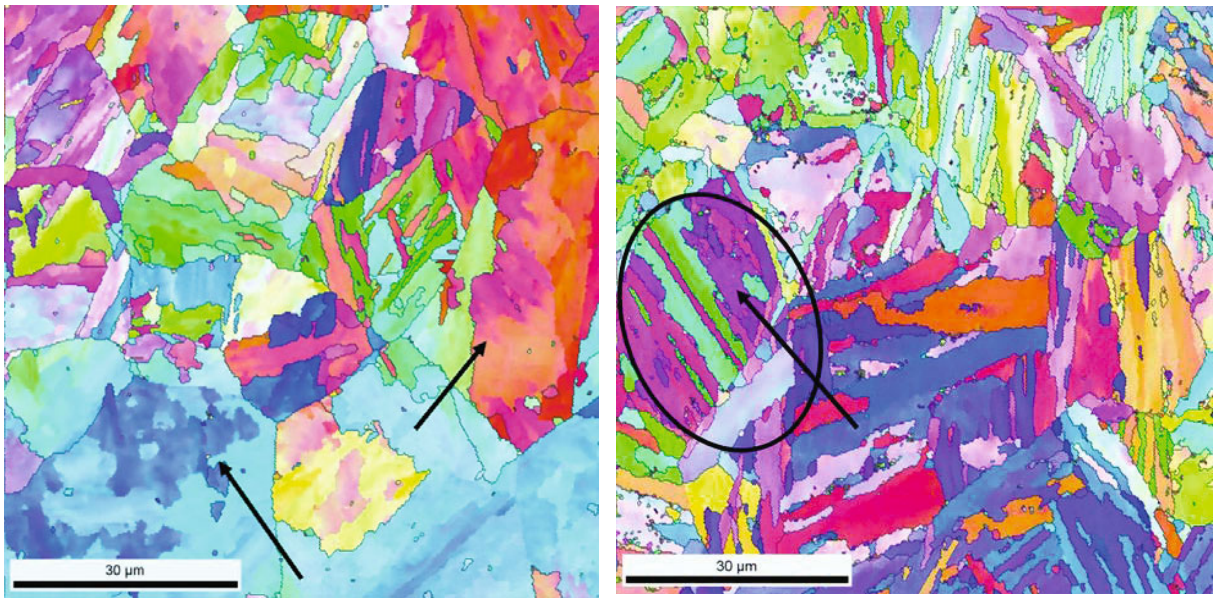

(a) (b)

Figure 18. Different bainitic microstructure sizes under different controlled cooling rates detected with EBSD techniques. (a) slow cooling rate; (b) fast cooling rate.

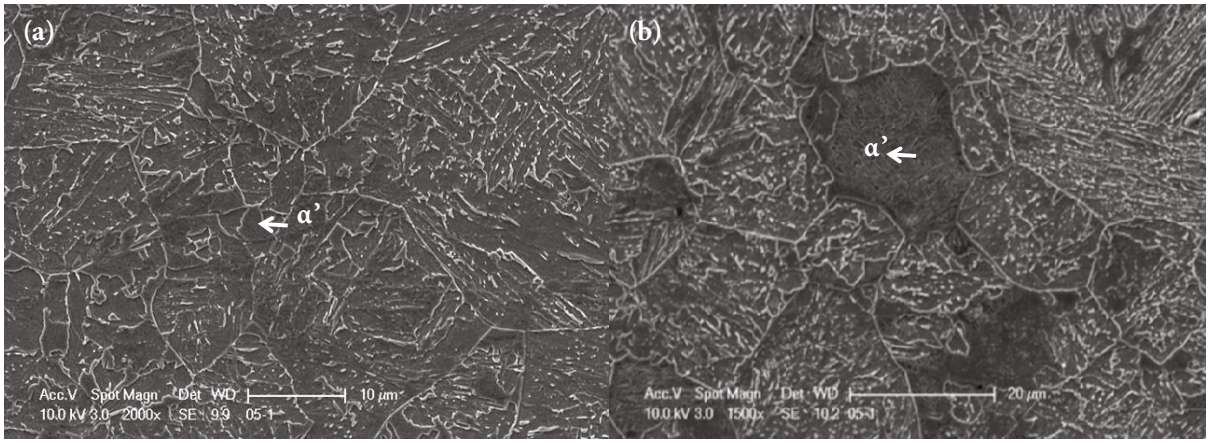

Figure 19. Isothermally treated SEM microstructures.(a) 450°C, 4 minutes;(b) 450°C, 10 minutes.

Microalloying and Zinc-coated Advanced High Strength Steels

Over the past decade, the UTS of high strength dual-phase steels has risen from 590 MPA to 780 MPa commercially and to over 1180MPa experimentally. Much of this increase is due to the addition of Nb and/or V to the base compositions [25-27]. In this current work, 0.06 V, was added to a base composition containing 0.1 C-1.5 Mn plus either a 1.5 Mn - 0.5 Cr - 0.3 Mo or a 1.5 Mn - 0.25 Cr - 0.1 Mo base. It has been shown that the MAE provided four benefits: (i) increase the hardenability of the intercritically-formed austenite, thereby allowing less new ferrite to form on cooling; (ii) reduce the martensite island size, hence increasing the work hardening rate and stretch formability; (iii) strengthen the ferrite, and leading to overall higher strengths; and finally (iv) increase the tempering resistance of the bainite and other types of ferrite formed at 460°C, the temperature of the zinc pot. After intercritical annealing at 790°C and cooling to 460°C using several thermal paths, the strengths of the resulting DP steels are shown in Figure 20.

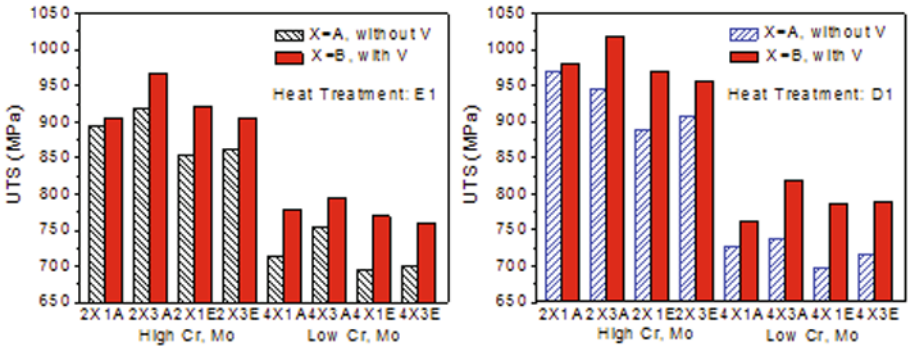

- **Gleeble heat treatments**

D1: 790C/60s, 15C/s, 460C/30s, 10C/s to RT
E1: 790C/60s, 15C/s, 250C/20s, 42C/s, 460C/30s, 10C/s to RT
E2: 790C/60s, 15C/s, 320C/20s, 42C/s, 460C/30s, 10C/s to RT
E3: 790C/60s, 15C/s, 390C/20s, 42C/s, 460C/30s, 10C/s to RT

Figure 20. Strength of Dual Phase Steels using different thermal paths in CGL simulations

Several interesting observations can be made concerning Figure 20. One is that the small vanadium addition had a large effect on the final UTS of up to 66 MPa for the higher alloyed version of the DP steel, and up to 84MPa in the lower alloy version. Another important observation is the obvious importance of the higher levels of Cr and Mo in the higher alloy version. Still another is the higher effectiveness of the V in the lower alloy version than the higher alloy version. The addition of the vanadium led to higher strengths with only a slight lowering of elongation and reduction in area. Finally, the sheared edge ductility or hole expansion ratio properties of the V-bearing steel were similar to the V-free steel, but at higher strength levels in the V steel.

The engineering effectiveness of the advanced high strength steels is often given as the product of (UTS, MPa) X (TE, %). The higher the product, the more effective the steel. Using this approach, products falling between 10,000 and 18,000 are considered good DP steel properties, products between 18,000 and 22,000 are considered good TRIP steel properties, and over 22,000 considered Generation III properties. This product is shown in Figure 13 for the two DP steels used in this experiment. For the standard GI process D1, there are two conditions that are Gen III and six that are TRIP level properties. For the supercooled practice E1, there are four conditions with Gen III properties and ten with TRIP steel properties.

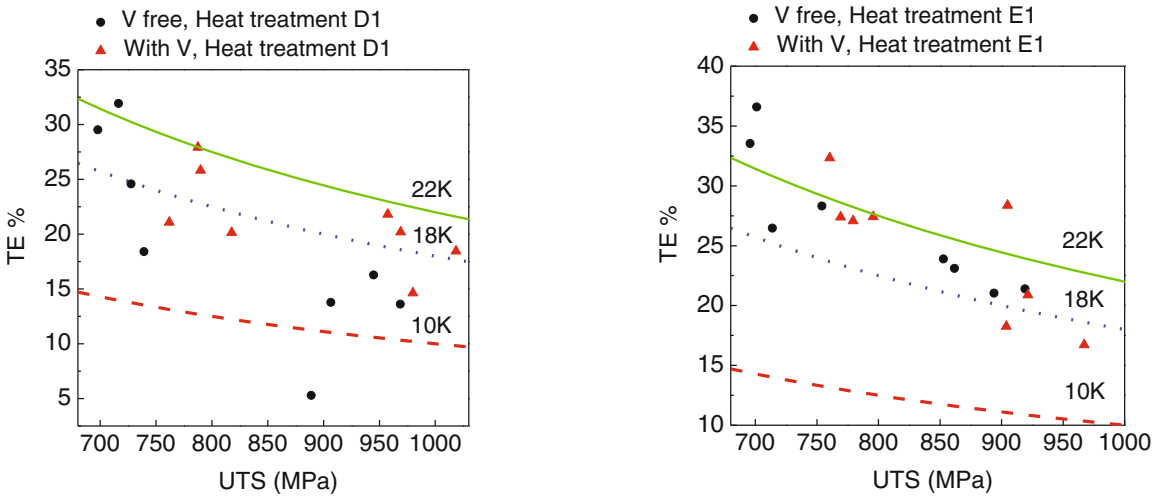

(a) (b)

Figure 21. (UTS x %TE) product data for experimental steels and processes, (a) process D1, (b) process E1. 10K dashed red, 18K dotted blue, and 22K solid green. By convention, 10K < DP < 18K; 18K < TRIP < 22K; and Gen III > 22K.

Summary and Conclusions

Vanadium is a valuable contributor to the performance of ferrite-pearlite HSLA steels. By taking advantage of grain refining and precipitation hardening that it can contribute, the use of vanadium in these products leads to improved strength and toughness.

The strength of bainitic ferrite in low carbon steels is directly related to its B50 temperature. Vanadium is a benefit here with its grain refining, solute drag and hardenability contribution.

Vanadium increases the strength of Dual-Phase steels with little penalty in ductility. The sheared edge ductility of the V-bearing steels was very good when considering the higher strength level.

In the experiments conducted, both the high alloy and the low alloy versions of the DP steels were processed with four different conditions of hot band microstructure(coiling temperature), and cold reduction and were also processed with four different thermal paths following the intercritical anneal. Several processing paths led to both TRIP and Generation III-level properties.

Acknowledgements

The author should like to thank Vanitec, Ltd. for providing financial support for the writing and presentation of this paper.

References

1. A. J. DeArdo, in Microalloying '95, ISS-AIME, Warrendale, 1995, 15.
2. A. J. DeArdo, Ironmaking and Steelmaking, Vol. 28, No. 2 (2001), pp.138-144.
3. A. J. DeArdo, "Niobium in Modern Steels," International Materials Reviews, Vol. 48, No. 6, (2003), pp.371-402.

4. A. LeBon et al., Microallying'75, pp90-99
5. I. Kozasu Microallying'75, pp120-135
6. T. Siwecki, et al., Microallying'95, Pittsburgh, ISS, Warrendale, 1995, pp 197-212
7. T vs strain E. J. Palmiere et al., in Low Carbon Steels for the 90's, edited by R. Asfahani and G. Tither, TMS AIME, Warrendale, 1993, pp121-130,
8. A. J. DeArdo and Mingjian Hua, Vanadium Microalloyed Steels: A Symposium in Memory of Michael Korchynsky, MS & T 2014.
9. L. J. Cuddy, Plastic Deformation of Metals, Academic Press, New York, 1975, pp. 129-140.
10. A. T. Davenport, et al., Met. Sci., Vol2, P104, 1968.
11. K. M. Tiitto et al., in Phase Transformations in Ferrous Alloys, TMS-AIME, Warrendale, 1984, pp. 281-292.
12. J. A. Todd, JOM, V43, 1991, pp. 45-48.
13. W. Gao, University of Pittsburgh, Unpublished Research , 1995
14. R. Lagneborg, et al., The Role of Vanadium in Microalloyed Steels, Vanitec, 2014, pp. 31-45.
15. A. Iza-Mendia, et al., Met Trans A, 2012.
16. A. D. Batte and R. W.K. Honeycombe, J. Iron Steel Inst, V211, 1973, p. 284
17. M. L. Santella, Ph. D. Thesis, University of Pittsburgh, 1981
18. R. L. Cryderman, in Proceedings of the Conference "Toward Improved Ductility and Toughness", Climax Molybdenum Company of Michigan, Ann Arbor, 1971, pp. 119-142.
19. K. J. Irvine and F. B. Pickering, J. Iron Steel Inst., V187, 1957, p. 292.
20. M. K. Graef et al., in Accelerated Cooling of Steel, TMS-AIME, Warrendale, PA 1986, pp. 165-180.
21. T. Siwecki et al., ISIJ International, V50, 2010, pp. 760-767.
22. X. Liang, "The Complex Phase Transformation of Austenite in High Strength Linepipe Steels and its Influence on the Mechanical Properties", Ph. D. Thesis, University of Pittsburgh, 2012
23. X. Liang and A. J. DeArdo, in Seventh International Conference on Physical and Numerical Simulation of Materials Processing, 2013.
24. X. Liang et al., "The Design of Microstructure for Strength and Toughness in Low Carbon High Strength Bainite Using EBSD Techniques", Materials Science and Technology (MS&T) 2014 October 12-16, 2014, Pittsburgh, Pennsylvania, USA, pp.1411-1420.
25. Y. Gong, PhD Thesis, University of Pittsburgh, 2015
26. Yu Gong and A. J. DeArdo, in MS&T 2014, TMS-AIME, Warrendale, PA, 2014
27. Yu Gong and A. J. DeArdo, in Galvatech 2015, TMS-AIME, Warrendale, PA, 2015